

# Search for a $1^{-+}$ molecular state via $e^+e^- \rightarrow \gamma D_s^+ D_{s1}^- (2536) + c.c.$

M. Ablikim<sup>1</sup>, M. N. Achasov<sup>4,c</sup>, P. Adlarson<sup>76</sup>, O. Afedulidis<sup>3</sup>, X. C. Ai<sup>81</sup>, R. Aliberti<sup>35</sup>, A. Amoroso<sup>75A,75C</sup>, Y. Bai<sup>57</sup>, O. Bakina<sup>36</sup>, I. Balossino<sup>29A</sup>, Y. Ban<sup>46,h</sup>, H.-R. Bao<sup>64</sup>, V. Batozskaya<sup>1,44</sup>, K. Begzsuren<sup>32</sup>, N. Berger<sup>35</sup>, M. Berlowski<sup>44</sup>, M. Bertani<sup>28A</sup>, D. Bettoni<sup>29A</sup>, F. Bianchi<sup>75A,75C</sup>, E. Bianco<sup>75A,75C</sup>, A. Bortone<sup>75A,75C</sup>, I. Boyko<sup>36</sup>, R. A. Briere<sup>5</sup>, A. Brueggemann<sup>69</sup>, H. Cai<sup>77</sup>, X. Cai<sup>1,58</sup>, A. Calcaterra<sup>28A</sup>, G. F. Cao<sup>1,64</sup>, N. Cao<sup>1,64</sup>, S. A. Cetin<sup>62A</sup>, X. Y. Chai<sup>46,h</sup>, J. F. Chang<sup>1,58</sup>, G. R. Che<sup>43</sup>, Y. Z. Che<sup>1,58,64</sup>, G. Chelkov<sup>36,b</sup>, C. Chen<sup>43</sup>, C. H. Chen<sup>9</sup>, Chao Chen<sup>55</sup>, G. Chen<sup>1</sup>, H. S. Chen<sup>1,64</sup>, H. Y. Chen<sup>20</sup>, M. L. Chen<sup>1,58,64</sup>, S. J. Chen<sup>42</sup>, S. L. Chen<sup>45</sup>, S. M. Chen<sup>61</sup>, T. Chen<sup>1,64</sup>, X. R. Chen<sup>31,64</sup>, X. T. Chen<sup>1,64</sup>, Y. B. Chen<sup>1,58</sup>, Y. Q. Chen<sup>34</sup>, Z. J. Chen<sup>25,i</sup>, S. K. Choi<sup>10</sup>, G. Cibinetto<sup>29A</sup>, F. Cossio<sup>75C</sup>, J. J. Cui<sup>50</sup>, H. L. Dai<sup>1,58</sup>, J. P. Dai<sup>79</sup>, A. Dbeyssi<sup>18</sup>, R. E. de Boer<sup>3</sup>, D. Dedovich<sup>36</sup>, C. Q. Deng<sup>73</sup>, Z. Y. Deng<sup>1</sup>, A. Denig<sup>35</sup>, I. Denysenko<sup>36</sup>, M. Destefanis<sup>75A,75C</sup>, F. De Mori<sup>75A,75C</sup>, B. Ding<sup>67,1</sup>, X. X. Ding<sup>46,h</sup>, Y. Ding<sup>34</sup>, Y. Ding<sup>40</sup>, J. Dong<sup>1,58</sup>, L. Y. Dong<sup>1,64</sup>, M. Y. Dong<sup>1,58,64</sup>, X. Dong<sup>77</sup>, M. C. Du<sup>1</sup>, S. X. Du<sup>81</sup>, Y. Y. Duan<sup>55</sup>, Z. H. Duan<sup>42</sup>, P. Egorov<sup>36,b</sup>, G. F. Fan<sup>42</sup>, J. J. Fan<sup>19</sup>, Y. H. Fan<sup>45</sup>, J. Fang<sup>59</sup>, J. Fang<sup>1,58</sup>, S. S. Fang<sup>1,64</sup>, W. X. Fang<sup>1</sup>, Y. Q. Fang<sup>1,58</sup>, R. Farinelli<sup>29A</sup>, L. Fava<sup>75B,75C</sup>, F. Feldbauer<sup>3</sup>, G. Felici<sup>28A</sup>, C. Q. Feng<sup>72,58</sup>, J. H. Feng<sup>59</sup>, Y. T. Feng<sup>72,58</sup>, M. Fritsch<sup>3</sup>, C. D. Fu<sup>1</sup>, J. L. Fu<sup>64</sup>, Y. W. Fu<sup>1,64</sup>, H. Gao<sup>64</sup>, X. B. Gao<sup>41</sup>, Y. N. Gao<sup>46,h</sup>, Y. N. Gao<sup>19</sup>, Yang Gao<sup>72,58</sup>, S. Garbolino<sup>75C</sup>, I. Garzia<sup>29A,29B</sup>, P. T. Ge<sup>19</sup>, Z. W. Ge<sup>42</sup>, C. Geng<sup>59</sup>, E. M. Gersabeck<sup>68</sup>, A. Gilman<sup>70</sup>, K. Goetzen<sup>13</sup>, L. Gong<sup>40</sup>, W. X. Gong<sup>1,58</sup>, W. Gradl<sup>35</sup>, S. Gramigna<sup>29A,29B</sup>, M. Greco<sup>75A,75C</sup>, M. H. Gu<sup>1,58</sup>, Y. T. Gu<sup>15</sup>, C. Y. Guan<sup>1,64</sup>, A. Q. Guo<sup>31,64</sup>, L. B. Guo<sup>41</sup>, M. J. Guo<sup>50</sup>, R. P. Guo<sup>49</sup>, Y. P. Guo<sup>12,g</sup>, A. Guskov<sup>36,b</sup>, J. Gutierrez<sup>27</sup>, K. L. Han<sup>64</sup>, T. T. Han<sup>1</sup>, F. Hanisch<sup>3</sup>, X. Q. Hao<sup>19</sup>, F. A. Harris<sup>66</sup>, K. K. He<sup>55</sup>, K. L. He<sup>1,64</sup>, F. H. Heinsius<sup>3</sup>, C. H. Heinz<sup>35</sup>, Y. K. Heng<sup>1,58,64</sup>, C. Herold<sup>60</sup>, T. Holtmann<sup>3</sup>, P. C. Hong<sup>34</sup>, G. Y. Hou<sup>1,64</sup>, X. T. Hou<sup>1,64</sup>, Y. R. Hou<sup>64</sup>, Z. L. Hou<sup>1</sup>, B. Y. Hu<sup>59</sup>, H. M. Hu<sup>1,64</sup>, J. F. Hu<sup>56,j</sup>, Q. P. Hu<sup>72,58</sup>, S. L. Hu<sup>12,g</sup>, T. Hu<sup>1,58,64</sup>, Y. Hu<sup>1</sup>, G. S. Huang<sup>72,58</sup>, K. X. Huang<sup>59</sup>, L. Q. Huang<sup>31,64</sup>, P. Huang<sup>42</sup>, X. T. Huang<sup>50</sup>, Y. P. Huang<sup>1</sup>, Y. S. Huang<sup>59</sup>, T. Hussain<sup>74</sup>, F. Hölzken<sup>3</sup>, N. Hüsken<sup>35</sup>, N. in der Wiesche<sup>69</sup>, J. Jackson<sup>27</sup>, S. Janchiv<sup>32</sup>, Q. Ji<sup>1</sup>, Q. P. Ji<sup>19</sup>, W. Ji<sup>1,64</sup>, X. B. Ji<sup>1,64</sup>, X. L. Ji<sup>1,58</sup>, Y. Y. Ji<sup>50</sup>, X. Q. Jia<sup>50</sup>, Z. K. Jia<sup>72,58</sup>, D. Jiang<sup>1,64</sup>, H. B. Jiang<sup>77</sup>, P. C. Jiang<sup>46,h</sup>, S. S. Jiang<sup>39</sup>, T. J. Jiang<sup>16</sup>, X. S. Jiang<sup>1,58,64</sup>, Y. Jiang<sup>64</sup>, J. B. Jiao<sup>50</sup>, J. K. Jiao<sup>34</sup>, Z. Jiao<sup>23</sup>, S. Jin<sup>42</sup>, Y. Jin<sup>67</sup>, M. Q. Jing<sup>1,64</sup>, X. M. Jing<sup>64</sup>, T. Johansson<sup>76</sup>, S. Kabana<sup>33</sup>, N. Kalantar-Nayestanaki<sup>65</sup>, X. L. Kang<sup>9</sup>, X. S. Kang<sup>40</sup>, M. Kavatsyuk<sup>65</sup>, B. C. Ke<sup>81</sup>, V. Khachatryan<sup>27</sup>, A. Khoukaz<sup>69</sup>, R. Kiuchi<sup>1</sup>, O. B. Kolcu<sup>62A</sup>, B. Kopf<sup>3</sup>, M. Kuessner<sup>3</sup>, X. Kui<sup>1,64</sup>, N. Kumar<sup>26</sup>, A. Kupsc<sup>44,76</sup>, W. Kühn<sup>37</sup>, W. N. Lan<sup>19</sup>, T. T. Lei<sup>72,58</sup>, Z. H. Lei<sup>72,58</sup>, M. Lellmann<sup>35</sup>, T. Lenz<sup>35</sup>, C. Li<sup>47</sup>, C. Li<sup>43</sup>, C. H. Li<sup>39</sup>, Cheng Li<sup>72,58</sup>, D. M. Li<sup>81</sup>, F. Li<sup>1,58</sup>, G. Li<sup>1</sup>, H. B. Li<sup>1,64</sup>, H. J. Li<sup>19</sup>, H. N. Li<sup>56,j</sup>, Hui Li<sup>43</sup>, J. R. Li<sup>61</sup>, J. S. Li<sup>59</sup>, K. Li<sup>1</sup>, K. L. Li<sup>19</sup>, L. J. Li<sup>1,64</sup>, Lei Li<sup>48</sup>, M. H. Li<sup>43</sup>, P. L. Li<sup>64</sup>, P. R. Li<sup>38,k,l</sup>, Q. M. Li<sup>1,64</sup>, Q. X. Li<sup>50</sup>, R. Li<sup>17,31</sup>, T. Li<sup>50</sup>, T. Y. Li<sup>43</sup>, W. D. Li<sup>1,64</sup>, W. G. Li<sup>1,a</sup>, X. Li<sup>1,64</sup>, X. H. Li<sup>72,58</sup>, X. L. Li<sup>50</sup>, X. Y. Li<sup>1,8</sup>, X. Z. Li<sup>59</sup>, Y. Li<sup>19</sup>, Y. G. Li<sup>46,h</sup>, Z. J. Li<sup>59</sup>, Z. Y. Li<sup>79</sup>, C. Liang<sup>42</sup>, H. Liang<sup>72,58</sup>, Y. F. Liang<sup>54</sup>, Y. T. Liang<sup>31,64</sup>, G. R. Liao<sup>14</sup>, Y. P. Liao<sup>1,64</sup>, J. Libby<sup>26</sup>, A. Limphirat<sup>60</sup>, C. C. Lin<sup>55</sup>, C. X. Lin<sup>64</sup>, D. X. Lin<sup>31,64</sup>, T. Lin<sup>1</sup>, B. J. Liu<sup>1</sup>, B. X. Liu<sup>77</sup>, C. Liu<sup>34</sup>, C. X. Liu<sup>1</sup>, F. Liu<sup>1</sup>, F. H. Liu<sup>53</sup>, Feng Liu<sup>6</sup>, G. M. Liu<sup>56,j</sup>, H. Liu<sup>38,k,l</sup>, H. B. Liu<sup>15</sup>, H. H. Liu<sup>1</sup>, H. M. Liu<sup>1,64</sup>, Huihui Liu<sup>21</sup>, J. B. Liu<sup>72,58</sup>, K. Liu<sup>38,k,l</sup>, K. Y. Liu<sup>40</sup>, Ke Liu<sup>22</sup>, L. Liu<sup>72,58</sup>, L. C. Liu<sup>43</sup>, Lu Liu<sup>43</sup>, M. H. Liu<sup>12,g</sup>, P. L. Liu<sup>1</sup>, Q. Liu<sup>64</sup>, S. B. Liu<sup>72,58</sup>, T. Liu<sup>12,g</sup>, W. K. Liu<sup>43</sup>, W. M. Liu<sup>72,58</sup>, X. Liu<sup>39</sup>, X. Liu<sup>38,k,l</sup>, Y. Liu<sup>81</sup>, Y. Liu<sup>38,k,l</sup>, Y. B. Liu<sup>43</sup>, Z. A. Liu<sup>1,58,64</sup>, Z. D. Liu<sup>9</sup>, Z. Q. Liu<sup>50</sup>, X. C. Lou<sup>1,58,64</sup>, F. X. Lu<sup>59</sup>, H. J. Lu<sup>23</sup>, J. G. Lu<sup>1,58</sup>, Y. Lu<sup>7</sup>, Y. P. Lu<sup>1,58</sup>, Z. H. Lu<sup>1,64</sup>, C. L. Luo<sup>41</sup>, J. R. Luo<sup>59</sup>, M. X. Luo<sup>80</sup>, T. Luo<sup>12,g</sup>, X. L. Luo<sup>1,58</sup>, X. R. Lyu<sup>64</sup>, Y. F. Lyu<sup>43</sup>, F. C. Ma<sup>40</sup>, H. Ma<sup>79</sup>, H. L. Ma<sup>1</sup>, J. L. Ma<sup>1,64</sup>, L. L. Ma<sup>50</sup>, L. R. Ma<sup>67</sup>, Q. M. Ma<sup>1</sup>, R. Q. Ma<sup>1,64</sup>, R. Y. Ma<sup>19</sup>, T. Ma<sup>72,58</sup>, X. T. Ma<sup>1,64</sup>, X. Y. Ma<sup>1,58</sup>, Y. M. Ma<sup>31</sup>, F. E. Maas<sup>18</sup>, I. MacKay<sup>70</sup>, M. Maggiora<sup>75A,75C</sup>, S. Malde<sup>70</sup>, Y. J. Mao<sup>46,h</sup>, Z. P. Mao<sup>1</sup>, S. Marcello<sup>75A,75C</sup>, Y. H. Meng<sup>64</sup>, Z. X. Meng<sup>67</sup>, J. G. Messchendorp<sup>13,65</sup>, G. Mezzadri<sup>29A</sup>, H. Miao<sup>1,64</sup>, T. J. Min<sup>42</sup>, R. E. Mitchell<sup>27</sup>, X. H. Mo<sup>1,58,64</sup>, B. Moses<sup>27</sup>, N. Yu. Muchnoi<sup>4,c</sup>, J. Muskalla<sup>35</sup>, Y. Nefedov<sup>36</sup>, F. Nerling<sup>18,e</sup>, L. S. Nie<sup>20</sup>, I. B. Nikolaev<sup>4,c</sup>, Z. Ning<sup>1,58</sup>, S. Nisar<sup>11,m</sup>, Q. L. Niu<sup>38,k,l</sup>, W. D. Niu<sup>55</sup>, Y. Niu<sup>50</sup>, S. L. Olsen<sup>10,64</sup>, Q. Ouyang<sup>1,58,64</sup>, S. Pacetti<sup>28B,28C</sup>, X. Pan<sup>55</sup>, Y. Pan<sup>57</sup>, A. Pathak<sup>10</sup>, Y. P. Pei<sup>72,58</sup>, M. Pelizaeus<sup>3</sup>, H. P. Peng<sup>72,58</sup>, Y. Y. Peng<sup>38,k,l</sup>, K. Peters<sup>13,e</sup>, J. L. Ping<sup>41</sup>, R. G. Ping<sup>1,64</sup>, S. Plura<sup>35</sup>, V. Prasad<sup>33</sup>, F. Z. Qi<sup>1</sup>, H. R. Qi<sup>61</sup>, M. Qi<sup>42</sup>, S. Qian<sup>1,58</sup>, W. B. Qian<sup>64</sup>, C. F. Qiao<sup>64</sup>, J. H. Qiao<sup>19</sup>, J. J. Qin<sup>73</sup>, L. Q. Qin<sup>14</sup>, L. Y. Qin<sup>72,58</sup>, X. P. Qin<sup>12,g</sup>, X. S. Qin<sup>50</sup>, Z. H. Qin<sup>1,58</sup>, J. F. Qiu<sup>1</sup>, Z. H. Qu<sup>73</sup>, C. F. Redmer<sup>35</sup>, K. J. Ren<sup>39</sup>, A. Rivetti<sup>75C</sup>, M. Rolo<sup>75C</sup>, G. Rong<sup>1,64</sup>, Ch. Rosner<sup>18</sup>, M. Q. Ruan<sup>1,58</sup>, S. N. Ruan<sup>43</sup>, N. Salone<sup>44</sup>, A. Sarantsev<sup>36,d</sup>, Y. Schelhaas<sup>35</sup>, K. Schoenning<sup>76</sup>, M. Scodggio<sup>29A</sup>, K. Y. Shan<sup>12,g</sup>, W. Shan<sup>24</sup>, X. Y. Shan<sup>72,58</sup>, Z. J. Shang<sup>38,k,l</sup>, J. F. Shangguan<sup>16</sup>, L. G. Shao<sup>1,64</sup>, M. Shao<sup>72,58</sup>, C. P. Shen<sup>12,g</sup>, H. F. Shen<sup>1,8</sup>, W. H. Shen<sup>64</sup>, X. Y. Shen<sup>1,64</sup>, B. A. Shi<sup>64</sup>, H. Shi<sup>72,58</sup>, J. L. Shi<sup>12,g</sup>, J. Y. Shi<sup>1</sup>, S. Y. Shi<sup>73</sup>, X. Shi<sup>1,58</sup>, J. J. Song<sup>19</sup>, T. Z. Song<sup>59</sup>, W. M. Song<sup>34,1</sup>, Y. J. Song<sup>12,g</sup>, Y. X. Song<sup>46,h,n</sup>, S. Sosio<sup>75A,75C</sup>, S. Spataro<sup>75A,75C</sup>,

F. Stieler<sup>35</sup>, S. S. Su<sup>40</sup>, Y. J. Su<sup>64</sup>, G. B. Sun<sup>77</sup>, G. X. Sun<sup>1</sup>, H. Sun<sup>64</sup>, H. K. Sun<sup>1</sup>, J. F. Sun<sup>19</sup>, K. Sun<sup>61</sup>, L. Sun<sup>77</sup>, S. S. Sun<sup>1,64</sup>, T. Sun<sup>51,f</sup>, Y. J. Sun<sup>72,58</sup>, Y. Z. Sun<sup>1</sup>, Z. Q. Sun<sup>1,64</sup>, Z. T. Sun<sup>50</sup>, C. J. Tang<sup>54</sup>, G. Y. Tang<sup>1</sup>, J. Tang<sup>59</sup>, M. Tang<sup>72,58</sup>, Y. A. Tang<sup>77</sup>, L. Y. Tao<sup>73</sup>, M. Tat<sup>70</sup>, J. X. Teng<sup>72,58</sup>, V. Thoren<sup>76</sup>, W. H. Tian<sup>59</sup>, Y. Tian<sup>31,64</sup>, Z. F. Tian<sup>77</sup>, I. Uman<sup>62B</sup>, Y. Wan<sup>55</sup>, S. J. Wang<sup>50</sup>, B. Wang<sup>1</sup>, Bo Wang<sup>72,58</sup>, C. Wang<sup>19</sup>, D. Y. Wang<sup>46,h</sup>, H. J. Wang<sup>38,k,l</sup>, J. J. Wang<sup>77</sup>, J. P. Wang<sup>50</sup>, K. Wang<sup>1,58</sup>, L. L. Wang<sup>1</sup>, L. W. Wang<sup>34</sup>, M. Wang<sup>50</sup>, N. Y. Wang<sup>64</sup>, S. Wang<sup>12,g</sup>, S. Wang<sup>38,k,l</sup>, T. Wang<sup>12,g</sup>, T. J. Wang<sup>43</sup>, W. Wang<sup>59</sup>, W. Wang<sup>73</sup>, W. P. Wang<sup>35,58,72,o</sup>, X. Wang<sup>46,h</sup>, X. F. Wang<sup>38,k,l</sup>, X. J. Wang<sup>39</sup>, X. L. Wang<sup>12,g</sup>, X. N. Wang<sup>1</sup>, Y. Wang<sup>61</sup>, Y. D. Wang<sup>45</sup>, Y. F. Wang<sup>1,58,64</sup>, Y. H. Wang<sup>38,k,l</sup>, Y. L. Wang<sup>19</sup>, Y. N. Wang<sup>45</sup>, Y. Q. Wang<sup>1</sup>, Yaqian Wang<sup>17</sup>, Yi Wang<sup>61</sup>, Z. Wang<sup>1,58</sup>, Z. L. Wang<sup>73</sup>, Z. Y. Wang<sup>1,64</sup>, D. H. Wei<sup>14</sup>, F. Weidner<sup>69</sup>, S. P. Wen<sup>1</sup>, Y. R. Wen<sup>39</sup>, U. Wiedner<sup>3</sup>, G. Wilkinson<sup>70</sup>, M. Wolke<sup>76</sup>, L. Wollenberg<sup>3</sup>, C. Wu<sup>39</sup>, J. F. Wu<sup>1,8</sup>, L. H. Wu<sup>1</sup>, L. J. Wu<sup>1,64</sup>, Lianjie Wu<sup>19</sup>, X. Wu<sup>12,g</sup>, X. H. Wu<sup>34</sup>, Y. H. Wu<sup>55</sup>, Y. J. Wu<sup>31</sup>, Z. Wu<sup>1,58</sup>, L. Xia<sup>72,58</sup>, X. M. Xian<sup>39</sup>, B. H. Xiang<sup>1,64</sup>, T. Xiang<sup>46,h</sup>, D. Xiao<sup>38,k,l</sup>, G. Y. Xiao<sup>42</sup>, H. Xiao<sup>73</sup>, Y. L. Xiao<sup>12,g</sup>, Z. J. Xiao<sup>41</sup>, C. Xie<sup>42</sup>, X. H. Xie<sup>46,h</sup>, Y. Xie<sup>50</sup>, Y. G. Xie<sup>1,58</sup>, Y. H. Xie<sup>6</sup>, Z. P. Xie<sup>72,58</sup>, T. Y. Xing<sup>1,64</sup>, C. F. Xu<sup>1,64</sup>, C. J. Xu<sup>59</sup>, G. F. Xu<sup>1</sup>, M. Xu<sup>72,58</sup>, Q. J. Xu<sup>16</sup>, Q. N. Xu<sup>30</sup>, W. L. Xu<sup>67</sup>, X. P. Xu<sup>55</sup>, Y. Xu<sup>40</sup>, Y. C. Xu<sup>78</sup>, Z. S. Xu<sup>64</sup>, F. Yan<sup>12,g</sup>, L. Yan<sup>12,g</sup>, W. B. Yan<sup>72,58</sup>, W. C. Yan<sup>81</sup>, W. P. Yan<sup>19</sup>, X. Q. Yan<sup>1,64</sup>, H. J. Yang<sup>51,f</sup>, H. L. Yang<sup>34</sup>, H. X. Yang<sup>1</sup>, J. H. Yang<sup>42</sup>, R. J. Yang<sup>19</sup>, T. Yang<sup>1</sup>, Y. Yang<sup>12,g</sup>, Y. F. Yang<sup>43</sup>, Y. X. Yang<sup>1,64</sup>, Y. Z. Yang<sup>19</sup>, Z. W. Yang<sup>38,k,l</sup>, Z. P. Yao<sup>50</sup>, M. Ye<sup>1,58</sup>, M. H. Ye<sup>8</sup>, Junhao Yin<sup>43</sup>, Z. Y. You<sup>59</sup>, B. X. Yu<sup>1,58,64</sup>, C. X. Yu<sup>43</sup>, G. Yu<sup>13</sup>, J. S. Yu<sup>25,i</sup>, M. C. Yu<sup>40</sup>, T. Yu<sup>73</sup>, X. D. Yu<sup>46,h</sup>, C. Z. Yuan<sup>1,64</sup>, J. Yuan<sup>34</sup>, J. Yuan<sup>45</sup>, L. Yuan<sup>2</sup>, S. C. Yuan<sup>1,64</sup>, Y. Yuan<sup>1,64</sup>, Z. Y. Yuan<sup>59</sup>, C. X. Yue<sup>39</sup>, Ying Yue<sup>19</sup>, A. A. Zafar<sup>74</sup>, F. R. Zeng<sup>50</sup>, S. H. Zeng<sup>63A,63B,63C,63D</sup>, X. Zeng<sup>12,g</sup>, Y. Zeng<sup>25,i</sup>, Y. J. Zeng<sup>59</sup>, Y. J. Zeng<sup>1,64</sup>, X. Y. Zhai<sup>34</sup>, Y. C. Zhai<sup>50</sup>, Y. H. Zhan<sup>59</sup>, A. Q. Zhang<sup>1,64</sup>, B. L. Zhang<sup>1,64</sup>, B. X. Zhang<sup>1</sup>, D. H. Zhang<sup>43</sup>, G. Y. Zhang<sup>19</sup>, H. Zhang<sup>81</sup>, H. Zhang<sup>72,58</sup>, H. C. Zhang<sup>1,58,64</sup>, H. H. Zhang<sup>59</sup>, H. Q. Zhang<sup>1,58,64</sup>, H. R. Zhang<sup>72,58</sup>, H. Y. Zhang<sup>1,58</sup>, J. Zhang<sup>59</sup>, J. Zhang<sup>81</sup>, J. J. Zhang<sup>52</sup>, J. L. Zhang<sup>20</sup>, J. Q. Zhang<sup>41</sup>, J. S. Zhang<sup>12,g</sup>, J. W. Zhang<sup>1,58,64</sup>, J. X. Zhang<sup>38,k,l</sup>, J. Y. Zhang<sup>1</sup>, J. Z. Zhang<sup>1,64</sup>, Jianyu Zhang<sup>64</sup>, L. M. Zhang<sup>61</sup>, Lei Zhang<sup>42</sup>, P. Zhang<sup>1,64</sup>, Q. Zhang<sup>19</sup>, Q. Y. Zhang<sup>34</sup>, R. Y. Zhang<sup>38,k,l</sup>, S. H. Zhang<sup>1,64</sup>, Shulei Zhang<sup>25,i</sup>, X. M. Zhang<sup>1</sup>, X. Y. Zhang<sup>40</sup>, X. Y. Zhang<sup>50</sup>, Y. Zhang<sup>73</sup>, Y. Zhang<sup>1</sup>, Y. T. Zhang<sup>81</sup>, Y. H. Zhang<sup>1,58</sup>, Y. M. Zhang<sup>39</sup>, Yan Zhang<sup>72,58</sup>, Z. D. Zhang<sup>1</sup>, Z. H. Zhang<sup>1</sup>, Z. L. Zhang<sup>34</sup>, Z. X. Zhang<sup>19</sup>, Z. Y. Zhang<sup>43</sup>, Z. Y. Zhang<sup>77</sup>, Z. Z. Zhang<sup>45</sup>, Zh. Zh. Zhang<sup>19</sup>, G. Zhao<sup>1</sup>, J. Y. Zhao<sup>1,64</sup>, J. Z. Zhao<sup>1,58</sup>, L. Zhao<sup>1</sup>, Lei Zhao<sup>72,58</sup>, M. G. Zhao<sup>43</sup>, N. Zhao<sup>79</sup>, R. P. Zhao<sup>64</sup>, S. J. Zhao<sup>81</sup>, Y. B. Zhao<sup>1,58</sup>, Y. X. Zhao<sup>31,64</sup>, Z. G. Zhao<sup>72,58</sup>, A. Zhemchugov<sup>36,b</sup>, B. Zheng<sup>73</sup>, B. M. Zheng<sup>34</sup>, J. P. Zheng<sup>1,58</sup>, W. J. Zheng<sup>1,64</sup>, X. R. Zheng<sup>19</sup>, Y. H. Zheng<sup>64</sup>, B. Zhong<sup>41</sup>, X. Zhong<sup>59</sup>, H. Zhou<sup>35,50,o</sup>, J. Y. Zhou<sup>34</sup>, S. Zhou<sup>6</sup>, X. Zhou<sup>77</sup>, X. K. Zhou<sup>6</sup>, X. R. Zhou<sup>72,58</sup>, X. Y. Zhou<sup>39</sup>, Y. Z. Zhou<sup>12,g</sup>, Z. C. Zhou<sup>20</sup>, A. N. Zhu<sup>64</sup>, J. Zhu<sup>43</sup>, K. Zhu<sup>1</sup>, K. J. Zhu<sup>1,58,64</sup>, K. S. Zhu<sup>12,g</sup>, L. Zhu<sup>34</sup>, L. X. Zhu<sup>64</sup>, S. H. Zhu<sup>71</sup>, T. J. Zhu<sup>12,g</sup>, W. D. Zhu<sup>41</sup>, W. Z. Zhu<sup>19</sup>, Y. C. Zhu<sup>72,58</sup>, Z. A. Zhu<sup>1,64</sup>, J. H. Zou<sup>1</sup>, J. Zu<sup>72,58</sup>

(BESIII Collaboration)

<sup>1</sup> Institute of High Energy Physics, Beijing 100049, People's Republic of China

<sup>2</sup> Beihang University, Beijing 100191, People's Republic of China

<sup>3</sup> Bochum Ruhr-University, D-44780 Bochum, Germany

<sup>4</sup> Budker Institute of Nuclear Physics SB RAS (BINP), Novosibirsk 630090, Russia

<sup>5</sup> Carnegie Mellon University, Pittsburgh, Pennsylvania 15213, USA

<sup>6</sup> Central China Normal University, Wuhan 430079, People's Republic of China

<sup>7</sup> Central South University, Changsha 410083, People's Republic of China

<sup>8</sup> China Center of Advanced Science and Technology, Beijing 100190, People's Republic of China

<sup>9</sup> China University of Geosciences, Wuhan 430074, People's Republic of China

<sup>10</sup> Chung-Ang University, Seoul, 06974, Republic of Korea

<sup>11</sup> COMSATS University Islamabad, Lahore Campus, Defence Road, Off Raiwind Road, 54000 Lahore, Pakistan

<sup>12</sup> Fudan University, Shanghai 200433, People's Republic of China

<sup>13</sup> GSI Helmholtzcentre for Heavy Ion Research GmbH, D-64291 Darmstadt, Germany

<sup>14</sup> Guangxi Normal University, Guilin 541004, People's Republic of China

<sup>15</sup> Guangxi University, Nanning 530004, People's Republic of China

<sup>16</sup> Hangzhou Normal University, Hangzhou 310036, People's Republic of China

<sup>17</sup> Hebei University, Baoding 071002, People's Republic of China

<sup>18</sup> Helmholtz Institute Mainz, Staudinger Weg 18, D-55099 Mainz, Germany

<sup>19</sup> Henan Normal University, Xinxiang 453007, People's Republic of China

<sup>20</sup> Henan University, Kaifeng 475004, People's Republic of China

- <sup>21</sup> Henan University of Science and Technology, Luoyang 471003, People's Republic of China
- <sup>22</sup> Henan University of Technology, Zhengzhou 450001, People's Republic of China
- <sup>23</sup> Huangshan College, Huangshan 245000, People's Republic of China
- <sup>24</sup> Hunan Normal University, Changsha 410081, People's Republic of China
- <sup>25</sup> Hunan University, Changsha 410082, People's Republic of China
- <sup>26</sup> Indian Institute of Technology Madras, Chennai 600036, India
- <sup>27</sup> Indiana University, Bloomington, Indiana 47405, USA
- <sup>28</sup> INFN Laboratori Nazionali di Frascati, (A)INFN Laboratori Nazionali di Frascati, I-00044, Frascati, Italy; (B)INFN Sezione di Perugia, I-06100, Perugia, Italy; (C)University of Perugia, I-06100, Perugia, Italy
- <sup>29</sup> INFN Sezione di Ferrara, (A)INFN Sezione di Ferrara, I-44122, Ferrara, Italy; (B)University of Ferrara, I-44122, Ferrara, Italy
- <sup>30</sup> Inner Mongolia University, Hohhot 010021, People's Republic of China
- <sup>31</sup> Institute of Modern Physics, Lanzhou 730000, People's Republic of China
- <sup>32</sup> Institute of Physics and Technology, Peace Avenue 54B, Ulaanbaatar 13330, Mongolia
- <sup>33</sup> Instituto de Alta Investigación, Universidad de Tarapacá, Casilla 7D, Arica 1000000, Chile
- <sup>34</sup> Jilin University, Changchun 130012, People's Republic of China
- <sup>35</sup> Johannes Gutenberg University of Mainz, Johann-Joachim-Becher-Weg 45, D-55099 Mainz, Germany
- <sup>36</sup> Joint Institute for Nuclear Research, 141980 Dubna, Moscow region, Russia
- <sup>37</sup> Justus-Liebig-Universität Giessen, II. Physikalisches Institut, Heinrich-Buff-Ring 16, D-35392 Giessen, Germany
- <sup>38</sup> Lanzhou University, Lanzhou 730000, People's Republic of China
- <sup>39</sup> Liaoning Normal University, Dalian 116029, People's Republic of China
- <sup>40</sup> Liaoning University, Shenyang 110036, People's Republic of China
- <sup>41</sup> Nanjing Normal University, Nanjing 210023, People's Republic of China
- <sup>42</sup> Nanjing University, Nanjing 210093, People's Republic of China
- <sup>43</sup> Nankai University, Tianjin 300071, People's Republic of China
- <sup>44</sup> National Centre for Nuclear Research, Warsaw 02-093, Poland
- <sup>45</sup> North China Electric Power University, Beijing 102206, People's Republic of China
- <sup>46</sup> Peking University, Beijing 100871, People's Republic of China
- <sup>47</sup> Qufu Normal University, Qufu 273165, People's Republic of China
- <sup>48</sup> Renmin University of China, Beijing 100872, People's Republic of China
- <sup>49</sup> Shandong Normal University, Jinan 250014, People's Republic of China
- <sup>50</sup> Shandong University, Jinan 250100, People's Republic of China
- <sup>51</sup> Shanghai Jiao Tong University, Shanghai 200240, People's Republic of China
- <sup>52</sup> Shanxi Normal University, Linfen 041004, People's Republic of China
- <sup>53</sup> Shanxi University, Taiyuan 030006, People's Republic of China
- <sup>54</sup> Sichuan University, Chengdu 610064, People's Republic of China
- <sup>55</sup> Soochow University, Suzhou 215006, People's Republic of China
- <sup>56</sup> South China Normal University, Guangzhou 510006, People's Republic of China
- <sup>57</sup> Southeast University, Nanjing 211100, People's Republic of China
- <sup>58</sup> State Key Laboratory of Particle Detection and Electronics, Beijing 100049, Hefei 230026, People's Republic of China
- <sup>59</sup> Sun Yat-Sen University, Guangzhou 510275, People's Republic of China
- <sup>60</sup> Suranaree University of Technology, University Avenue 111, Nakhon Ratchasima 30000, Thailand
- <sup>61</sup> Tsinghua University, Beijing 100084, People's Republic of China
- <sup>62</sup> Turkish Accelerator Center Particle Factory Group, (A)Istinye University, 34010, Istanbul, Turkey; (B)Near East University, Nicosia, North Cyprus, 99138, Mersin 10, Turkey
- <sup>63</sup> University of Bristol, H H Wills Physics Laboratory, Tyndall Avenue, Bristol, BS8 1TL, UK
- <sup>64</sup> University of Chinese Academy of Sciences, Beijing 100049, People's Republic of China
- <sup>65</sup> University of Groningen, NL-9747 AA Groningen, The Netherlands
- <sup>66</sup> University of Hawaii, Honolulu, Hawaii 96822, USA
- <sup>67</sup> University of Jinan, Jinan 250022, People's Republic of China
- <sup>68</sup> University of Manchester, Oxford Road, Manchester, M13 9PL, United Kingdom
- <sup>69</sup> University of Muenster, Wilhelm-Klemm-Strasse 9, 48149 Muenster, Germany

<sup>70</sup> *University of Oxford, Keble Road, Oxford OX13RH, United Kingdom*

<sup>71</sup> *University of Science and Technology Liaoning, Anshan 114051, People's Republic of China*

<sup>72</sup> *University of Science and Technology of China, Hefei 230026, People's Republic of China*

<sup>73</sup> *University of South China, Hengyang 421001, People's Republic of China*

<sup>74</sup> *University of the Punjab, Lahore-54590, Pakistan*

<sup>75</sup> *University of Turin and INFN, (A)University of Turin, I-10125, Turin, Italy; (B)University of Eastern Piedmont, I-15121, Alessandria, Italy; (C)INFN, I-10125, Turin, Italy*

<sup>76</sup> *Uppsala University, Box 516, SE-75120 Uppsala, Sweden*

<sup>77</sup> *Wuhan University, Wuhan 430072, People's Republic of China*

<sup>78</sup> *Yantai University, Yantai 264005, People's Republic of China*

<sup>79</sup> *Yunnan University, Kunming 650500, People's Republic of China*

<sup>80</sup> *Zhejiang University, Hangzhou 310027, People's Republic of China*

<sup>81</sup> *Zhengzhou University, Zhengzhou 450001, People's Republic of China*

<sup>a</sup> *Deceased*

<sup>b</sup> *Also at the Moscow Institute of Physics and Technology, Moscow 141700, Russia*

<sup>c</sup> *Also at the Novosibirsk State University, Novosibirsk, 630090, Russia*

<sup>d</sup> *Also at the NRC "Kurchatov Institute", PNPI, 188300, Gatchina, Russia*

<sup>e</sup> *Also at Goethe University Frankfurt, 60323 Frankfurt am Main, Germany*

<sup>f</sup> *Also at Key Laboratory for Particle Physics, Astrophysics and Cosmology, Ministry of Education; Shanghai Key Laboratory for Particle Physics and Cosmology; Institute of Nuclear and Particle Physics, Shanghai 200240, People's Republic of China*

<sup>g</sup> *Also at Key Laboratory of Nuclear Physics and Ion-beam Application (MOE) and Institute of Modern Physics, Fudan University, Shanghai 200443, People's Republic of China*

<sup>h</sup> *Also at State Key Laboratory of Nuclear Physics and Technology, Peking University, Beijing 100871, People's Republic of China*

<sup>i</sup> *Also at School of Physics and Electronics, Hunan University, Changsha 410082, China*

<sup>j</sup> *Also at Guangdong Provincial Key Laboratory of Nuclear Science, Institute of Quantum Matter, South China Normal University, Guangzhou 510006, China*

<sup>k</sup> *Also at MOE Frontiers Science Center for Rare Isotopes, Lanzhou University, Lanzhou 730000, People's Republic of China*

<sup>l</sup> *Also at Lanzhou Center for Theoretical Physics, Lanzhou University, Lanzhou 730000, People's Republic of China*

<sup>m</sup> *Also at the Department of Mathematical Sciences, IBA, Karachi 75270, Pakistan*

<sup>n</sup> *Also at Ecole Polytechnique Federale de Lausanne (EPFL), CH-1015 Lausanne, Switzerland*

<sup>o</sup> *Also at Helmholtz Institute Mainz, Staudinger Weg 18, D-55099 Mainz, Germany*

(Dated: March 17, 2025)

We search, for the first time, for an exotic molecular state with quantum numbers  $J^{PC} = 1^{-+}$ , called  $X$ , via the process  $e^+e^- \rightarrow \gamma D_s^+ D_{s1}^-(2536) + c.c.$  using data samples corresponding to a luminosity of  $5.8 \text{ fb}^{-1}$  across center-of-mass energies from 4.612 to 4.951 GeV, collected with the BESIII detector operating at the BEPCII collider. No statistically significant signal is observed. The upper limits on the product of cross-section and branching fraction  $\sigma(e^+e^- \rightarrow \gamma X) \cdot \mathcal{B}(X \rightarrow D_s^+ D_{s1}^-(2536) + c.c.)$  at 90% confidence level are reported for each energy point, assuming the  $X$  mass to be 4.503 GeV/ $c^2$  and the width 25, 50, 75, and 100 MeV, respectively.

## I. INTRODUCTION

Since their discovery two decades ago [1], the charmonium-like states, known as XYZ, have enormously broadened our understanding of the hadronic mass spectrum. Unlike the conventional charmonium states, which are composed of charm quark anti-quark pairs ( $c\bar{c}$ ), the XYZ states are believed to present a more complex internal structure, including e.g. tetraquark, molecule, or hybrid. Therefore, they provide additional information which goes beyond the traditional  $c\bar{c}$  systems. The inves-

tigation of their spectrum, quantum numbers, production rate, and decays can shed light on the mechanisms of the strong interaction.

Since the charmonium-like states have the same quantum numbers as the charmonium states, they are difficult to be distinguished. For instance, the  $X(3872)$  was first observed in the  $B^\pm \rightarrow K^\pm \pi^+ \pi^- J/\psi$  decay by Belle [2] in 2003 and subsequently confirmed by several other experiments [3–5]. While  $X(3872)$  is believed as the first exotic charmonium-like particle [6–12], there remains a long-standing debate about whether it could instead be

the conventional  $\chi_{c1}(2P)$  state [9]. Similarly, the vector state  $Y(4230)$ , which was observed and subsequently confirmed in its decay to  $\pi^+\pi^-J/\psi$  [13–15]; there are ongoing arguments suggesting that it could be the charmonium  $\psi(4S)$  state [21–24], or an exotic state [16–20].

One possible way to bypass the aforementioned difficulty is to search for states that are “more exotic than the other exotic states”. The  $Z_c^\pm(3900)$  [25] is one kind of these states since it is charged and contains a  $c\bar{c}$  component. In between the light meson states, the  $\pi_1(1400)$  [26–30],  $\pi_1(1600)$  [31, 32], and  $\eta_1(1855)$  [33] are considered exotic states due to their unusual quantum numbers  $J^{PC} = 1^{-+}$ , indicating non- $q\bar{q}$  quark components. Exotic states with unusual quantum numbers have been found only in the light hadron spectrum, and up till now, no similar states have been discovered in the charmonium energy region, even if they are allowed by QCD. Ref. [34] discusses the possibility that heavy-light meson states, such as  $\bar{D}D_1(2420)$  and its charge conjugate (*c.c.*), can couple to states with exotic quantum numbers  $J^{PC} = 1^{-+}$  in *S*-wave. Similarly, this can also be extended to *D*-mesons with a strange quark, suggesting potential heavier exotic  $1^{-+}$  states near the  $D_s^+D_{s1}^-(2536)$  threshold. Throughout this paper without specification, the charge conjugated mode is implied.

In this paper, the process  $e^+e^- \rightarrow \gamma D_s^+ D_{s1}^-(2536)$  has been used to search for a molecular  $1^{-+}$  state *X*, formed by  $D_s^+ D_{s1}^-(2536)$ . This has been done using twelve data samples with center-of-mass (c.m.) energies ( $\sqrt{s}$ ) ranging from 4.612 to 4.951 GeV [35], corresponding to an integrated luminosity of  $5.8 \text{ fb}^{-1}$ . The values of c.m. energy and luminosity are listed in Table I.

## II. BESIII DETECTOR AND MONTE CARLO SIMULATION

The BESIII detector [36] records symmetric  $e^+e^-$  collisions provided by the BEPCII storage ring [37] in the c.m. energy range from 1.84 to 4.95 GeV, with a peak luminosity of  $1.1 \times 10^{33} \text{ cm}^{-2}\text{s}^{-1}$  achieved at  $\sqrt{s} = 3.773 \text{ GeV}$ . BESIII has collected large data samples in this energy region [37]. The cylindrical core of the BESIII detector covers 93% of the full solid angle and consists of a helium-based multilayer drift chamber (MDC), a plastic scintillator time-of-flight system (TOF), and a CsI(Tl) electromagnetic calorimeter (EMC), which are all enclosed in a superconducting solenoid magnet providing a 1.0 T magnetic field. The solenoid is supported by an octagonal flux-return yoke with resistive plate counter muon identification modules interleaved with steel. The charged-particle momentum resolution at 1 GeV/*c* is 0.5%, and the  $dE/dx$  resolution is 6% for electrons from Bhabha scattering. The EMC measures photon energies with a resolution of 2.5% (5%) at 1 GeV in the barrel (end cap) region. The time resolution in the TOF barrel region is 68 ps, while that in the end cap region is 110 ps. The end cap TOF system was upgraded in 2015 using multi-

gap resistive plate chamber technology, providing a time resolution of 60 ps, which benefits the total amount of the data used in this analysis [38].

Simulated data samples produced with a GEANT4-based [39] Monte Carlo (MC) package, which includes the geometric description of the BESIII detector [40] and the detector response, are used to determine the detection efficiencies and estimate backgrounds. The simulation models the beam energy spread and ISR in the  $e^+e^-$  annihilation with the KKMC generator [41]. The inclusive MC sample includes the production of open charm processes, the ISR production of vector charmonium(-like) states, and the continuum processes incorporated in KKMC [41]. All the known particle decays are modeled with EVTGEN [42] using the branching fractions either taken from the Particle Data Group (PDG) [43] or estimated with LUNDCHARM [44]. The final state radiation (FSR) from charged final state particles is incorporated using the PHOTOS package [45].

We generate 200,000 signal MC events of  $e^+e^- \rightarrow \gamma X$  and  $X \rightarrow D_s^+ D_{s1}^-(2536)$  at each c.m. energy and each hypothetical *X*'s width with uniform phase space (PHSP) distribution. The *X*'s mass ( $M_X$ ) is set to the  $D_s^+ D_{s1}^-(2536)$  mass threshold  $4.503 \text{ GeV}/c^2$ , based on the molecule assumption that its mass should be very close to, perhaps a few MeV lower than, this threshold [34]; its width ( $\Gamma_X$ ) is set to 25, 50, 75, and 100 MeV, reflecting the widths of the other charmonium-like states. We generate the  $D_s^+ \rightarrow K^+ K^- \pi^+$  decay based on the amplitude analysis results from Refs. [46–48], and the  $D_s^+ \rightarrow K_S^0 K^+$  and  $K_S^0 \rightarrow \pi^+ \pi^-$  decays according to the PHSP distribution. We generate  $D_{s1}^-(2536) \rightarrow \bar{D}^{*0} K^-$  process via VVS-PWAVE model [42], with inclusive decays of  $\bar{D}^{*0}$  following the world-averaged branching fractions [43], where  $\bar{D}^{*0}$  decays 64.7% into  $\bar{D}^0 \pi^0$  and 35.3% into  $\bar{D}^0 \gamma$ . The cross section line shape is assumed to be proportional to  $E_\gamma^3/s$  [49], where  $E_\gamma$  is the energy of the radiative photon. This information is used to obtain the radiative correction factor and detection efficiency.

## III. PRIMARY EVENT SELECTION

We employ a partial reconstruction method for the signal process  $e^+e^- \rightarrow \gamma D_s^+ D_{s1}^-(2536)$ ,  $D_{s1}^-(2536) \rightarrow \bar{D}^{*0} K^-$  to achieve higher efficiency. This method involves reconstructing the  $\gamma$ ,  $D_s^+$ , and a bachelor  $K^-$  from the  $D_{s1}^-(2536)$  decay. The  $D_{s1}^-(2536)$  and its daughter particle  $\bar{D}^{*0}$  are searched for in the recoiling mass spectrum of the  $\gamma D_s^+$  and  $\gamma D_s^+ K^-$  candidates, respectively. The  $D_s^+$  meson is reconstructed via  $K^+ K^- \pi^+$  or  $K_S^0 K^+$  with  $K_S^0 \rightarrow \pi^+ \pi^-$ .

Photon candidates are identified using showers in the EMC. The deposited energy of a shower must be greater than 25 MeV in the barrel region ( $|\cos\theta| < 0.80$ ) or greater than 50 MeV in the end cap region ( $0.86 < |\cos\theta| < 0.92$ ). Here  $\theta$  is the polar angle with respect to the *z*-axis, the symmetry axis of the MDC. To ex-

clude showers that originate from charged tracks, the angle subtended by the EMC shower and the position of the closest charged track at the EMC must be greater than 10 degrees as measured from the interaction point (IP). To suppress the electronic noise and the showers unrelated to the event, the difference between the EMC time and the event start time is required to be within  $[0, 700]$  ns. The number of photons per event is required to be at least one.

A charged track is reconstructed from the hits in the MDC. We require that each charged track not associated with the  $K_S^0$  must satisfy  $|\cos\theta| < 0.93$ , and the distance of the closest approach to the IP within 10 cm along the  $z$ -axis ( $V_z$ ), and less than 1 cm in the transverse plane. Particle identification (PID) for charged tracks combines measurements of the energy deposited in the MDC ( $dE/dx$ ) and the time-of-flight in the TOF to form likelihoods  $\mathcal{L}(h)$  ( $h = p, K, \pi$ ) for each hadron  $h$  hypothesis. Tracks are identified as  $K^\pm$  ( $\pi^\pm$ ) by comparing the likelihoods for the kaon and pion hypotheses, requiring  $\mathcal{L}(K) > \mathcal{L}(\pi)$  and  $\mathcal{L}(K) > 0$  ( $\mathcal{L}(\pi) > \mathcal{L}(K)$  and  $\mathcal{L}(\pi) > 0$ ).

Each  $K_S^0$  candidate is reconstructed from two oppositely charged tracks that satisfy  $|V_z| < 20$  cm and  $|\cos\theta| < 0.93$ . The two charged tracks are assigned as  $\pi^+\pi^-$  without imposing any PID criteria. They are constrained to originate from a common vertex and are required to have an invariant mass within  $|M_{\pi^+\pi^-} - m_{K_S^0}| < 9$  MeV/ $c^2$ , where  $m_{K_S^0}$  is the  $K_S^0$  nominal mass [43]. The decay length of the  $K_S^0$  candidate is required to be greater than twice the vertex resolution away from the IP.

The selected  $K^\pm$ ,  $\pi^\pm$ , and  $K_S^0$  candidates in an event are combined to reconstruct  $D_s^+ \rightarrow K^+K^-\pi^+$  or  $D_s^+ \rightarrow K_S^0K^+$ , denoted as the  $KK\pi$  or  $K_S^0K$  modes, respectively. At least one  $K^-$  with opposite charge to the  $D_s^+$  candidate is required. Only the decays containing the intermediate states  $\phi$  or  $\bar{K}^*(892)^0$  in the  $KK\pi$  mode are used to select the  $D_s^+$  candidates. The invariant mass of  $K^+K^-$  ( $K^+\pi^-$ ) is required to satisfy  $|M_{K^+K^-} - m_\phi| < 9$  MeV/ $c^2$  ( $|M_{K^+\pi^-} - m_{\bar{K}^*(892)^0}| < 66$  MeV/ $c^2$ ). The helicity angle of  $K^+$  in the  $K^+K^-$  ( $K^+\pi^-$ ) helicity frame is required to satisfy  $|\cos\theta| > 0.36$  ( $|\cos\theta| > 0.45$ ) to improve the significance of the  $D_s$  meson. As an example, Fig. 1 shows the invariant mass distributions of  $K^+K^-\pi^+$  ( $M_{K^+K^-\pi^+}$ ) and  $K_S^0K^+$  ( $M_{K_S^0K^+}$ ) at  $\sqrt{s} = 4.682$  GeV. The masses  $M_{K^+K^-\pi^+}$  and  $M_{K_S^0K^+}$  must satisfy  $|M_{K^+K^-\pi^+} - m_{D_s^+}| < 15$  MeV/ $c^2$  and  $|M_{K_S^0K^+} - m_{D_s^+}| < 19$  MeV/ $c^2$ , respectively. Here and hereafter,  $m_y$  ( $y = \phi, \bar{K}^*(892)^0, D_s^+$ ) denotes the respective nominal masses [43]. Since the resolutions and background levels are dependent on the c.m. energy, we categorize the data samples into three sets based on  $\sqrt{s}$  to optimize the event selection criteria:

- Set I: 4.612, 4.628, 4.641, 4.661, 4.682 GeV;
- Set II: 4.699, 4.740, 4.750, 4.781 GeV;

- Set III: 4.843, 4.918, 4.951 GeV.

Within a set, the resolutions and backgrounds are assumed to be similar for each energy point. To improve the resolution, the modified recoiling mass of  $\gamma D_s^+ K^-$  is defined as  $RM'_{D^*0} \equiv RM_{\gamma D_s^+ K^-} + M_{K^+K^-\pi^+} - m_{D_s^+}$ , with  $RM_{\gamma D_s^+ K^-} = \sqrt{(p_{c.m.} - p_\gamma - p_{D_s^+} - p_{K^-})^2}$ , in which  $p_{c.m.}$ ,  $p_\gamma$ ,  $p_{D_s^+}$ , and  $p_{K^-}$  are the four-momenta of the initial  $e^+e^-$  system, the radiative photon,  $D_s^+$ , and  $K^-$ , respectively. This definition is specified for the  $KK\pi$  mode, and a similar definition is applied for the  $K_S^0K$  mode. The interval range requirements of  $RM'_{D^*0}$  in the three sets are presented in Table II. These requirements are based on the Punzi method [50], optimizing the figure-of-merit (FOM)  $\epsilon/(\alpha/2 + \sqrt{B})$ , where  $\alpha = 3$  indicates the expected significance,  $\epsilon$  is the selection efficiency, and  $B$  is the number of background events from inclusive MC, as will be discussed in the next section. All possible combinations are retained for later analysis.

#### IV. BACKGROUND ANALYSIS AND SUPPRESSION

Based on [51], the  $e^+e^- \rightarrow D_s^{*+}D_{s1}^-(2536), D_s^{*+} \rightarrow \gamma D_s^+$  events constitute a peaking background and significantly contaminate the signal, since the final state is similar to the signal one. We require the invariant mass of  $\gamma D_s^+$  ( $M_{\gamma D_s^+}$ ) to satisfy  $|M_{\gamma D_s^+} - m_{D_s^{*+}}| > 9$  MeV/ $c^2$  to suppress this kind of background, as shown in Fig. 2, where  $m_{D_s^{*+}}$  is the nominal mass of  $D_s^{*+}$  [43] and the data sample at  $\sqrt{s} = 4.682$  GeV is presented as an example. It should be noted that suppressing this peaking background leads to a reduced efficiency at the energy values  $\sqrt{s} = 4.661$  and 4.682, as a result of the relatively larger overlap between the  $M_{\gamma D_s^+}$  distributions of the signal and background. After imposing all the above event selection criteria, the distributions of  $RM'_{D^*0}$  are shown in Fig. 3. We generate the exclusive MC samples of  $e^+e^- \rightarrow D_s^{*+}D_{s1}^-(2536)$  with  $D_s^{*+} \rightarrow \gamma D_s^+$  and  $e^+e^- \rightarrow D_s^+D_{s1}^-(2536)$  processes to estimate the background contamination. Their production cross-section line shapes and decay models are taken from the two BESIII measurements [51, 52]. The number of events for  $e^+e^- \rightarrow D_s^{*+}D_{s1}^-(2536), D_s^{*+} \rightarrow \gamma D_s^+$  at the 4.682 GeV energy is estimated to be 2.5 in the  $KK\pi$  mode and 0.5 in the  $K_S^0K$  mode by simulation. In addition, the backgrounds from  $e^+e^- \rightarrow (\gamma_{\text{ISR}})D_s^+D_{s1}^-(2536)$  are determined to be 1.2 events in the  $KK\pi$  and 0.3 in the  $K_S^0K$  mode at 4.682 GeV. Therefore, we ignore these two kinds of background in the cross-section measurements, and only consider their impact in the estimation of the systematic uncertainties.

To improve the resolution and further suppress the background, we perform a two-constraint (2C) kinematic fit to all the selected candidates, constraining  $M_{K^+K^-\pi^+}/K_S^0K^+$  to  $m_{D_s^+}$  and  $RM_{\gamma D_s^+ K^-}$  to  $m_{D^*0}$ . Here,

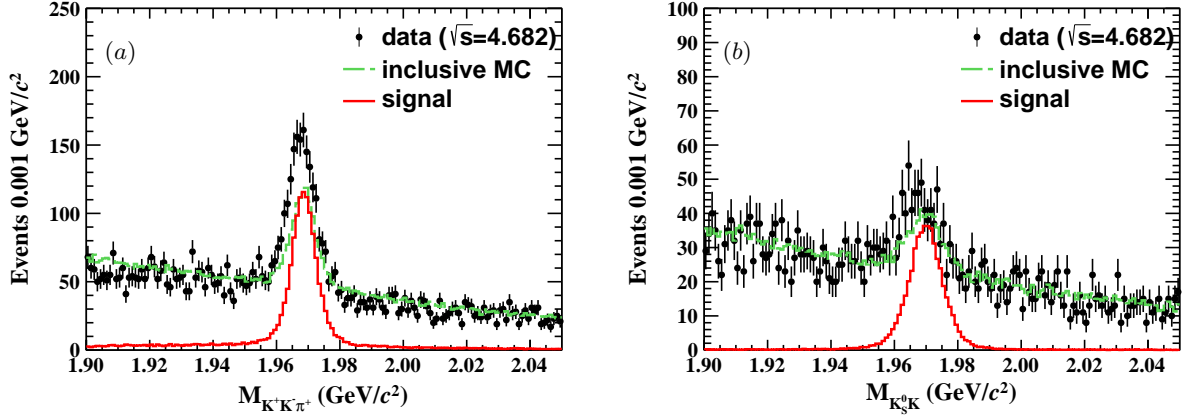


FIG. 1. Invariant mass distributions of  $M_{K+K-\pi^+}$  (a) and  $M_{K_S^0 K^+}$  (b) at  $\sqrt{s} = 4.682$  GeV. Dots with error bars represent data, the green dashed lines represent inclusive MC, red solid lines indicate the signal. The number of events in the inclusive MC simulation is normalized to match the data, while the signal is normalized arbitrarily.

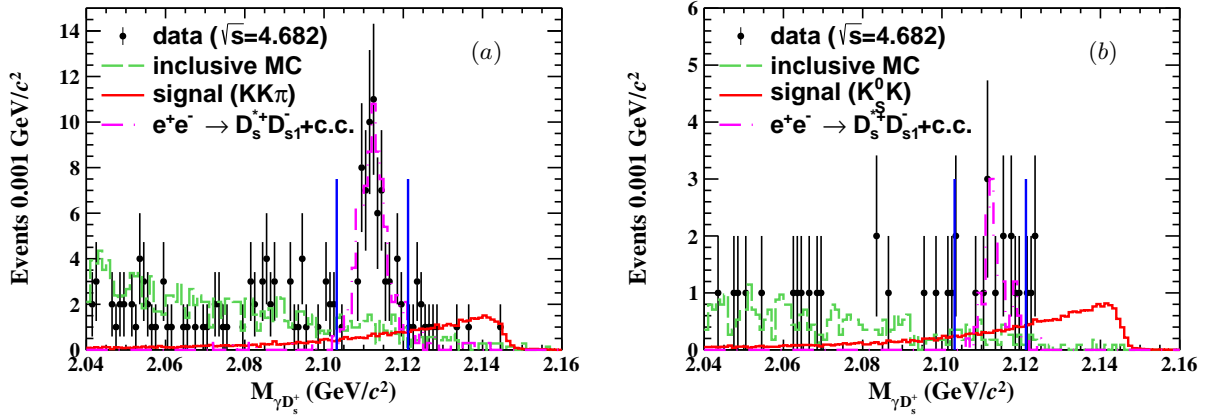


FIG. 2. Distributions of  $M_{\gamma D_s^+}$  at  $\sqrt{s} = 4.682$  GeV for the  $KK\pi$  mode (a) and the  $K_S^0 K$  mode (b) after the primary event selection. Dots with error bars indicate data, the green dashed lines indicate inclusive MC, red solid lines indicate signal, the pink dashed line indicates the peaking background from  $e^+e^- \rightarrow D_s^+ D_{s1}^- (2536), D_s^{*+} \rightarrow \gamma D_s^+$ , and blue solid lines indicate the mass range requirement for  $M_{\gamma D_s^+}$ .

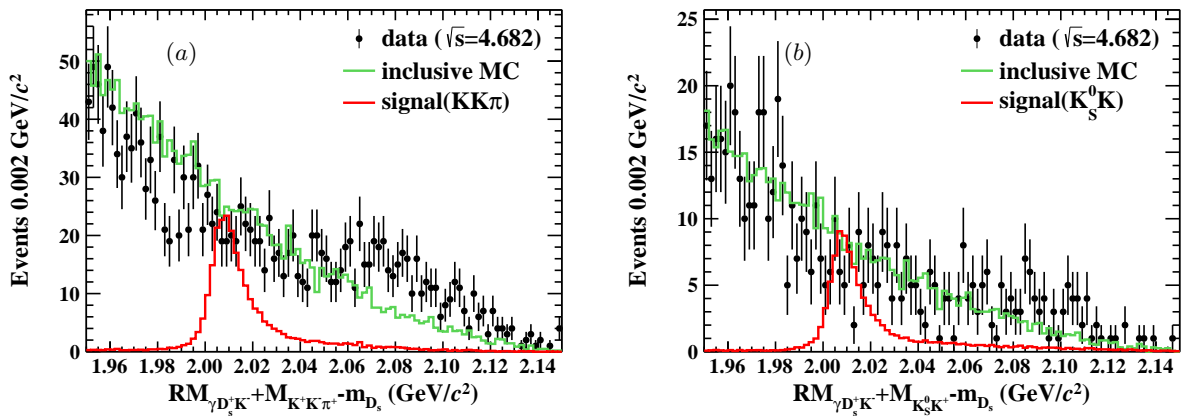


FIG. 3. Distributions of  $RM_{D^*0}$  at  $\sqrt{s} = 4.682$  GeV for the  $KK\pi$  mode (a) and the  $K_S^0 K$  mode (b) after the requirement of  $M_{\gamma D_s^+}$ . Dots with error bars indicate data, the green dashed lines indicate inclusive MC, red solid lines indicate signal. The number of events in the inclusive MC simulation is normalized to match the data, while the signal is normalized arbitrarily.

$m_{\bar{D}^{*0}}$  is the nominal mass of  $\bar{D}^{*0}$  [43]. If there are more than one combination in the event, the candidate with the lowest  $\chi^2$  value is chosen. To further suppress the backgrounds, we employed the Punzi method [50] to optimize the  $\chi^2$  requirements, as shown in Table II.

## V. SIGNAL YIELDS AND CROSS SECTIONS

To extract the number of signal events, we perform an unbinned two-dimensional simultaneous fit to the recoiling mass distribution of  $\gamma D_s^+$  ( $RM_{\gamma D_s^+}$ ) in the range (2.50, 2.60) GeV/ $c^2$  and of  $\gamma$  ( $RM_\gamma$ ) in the range (4.49,  $E'$ ) GeV/ $c^2$ , where  $E'$  represents  $\sqrt{s} - 0.025$  GeV (0.025 GeV is the minimum requirement for the photon deposited energy). The line-shapes of the  $D_{s1}^-(2536)$  and of the  $X$  states are described by the simulated MC shapes with  $M_X$  set to 4.503 GeV/ $c^2$  and  $\Gamma_X$  set to 50 MeV. For the subsequent study of the systematic uncertainties, additional MC samples are generated with  $\Gamma_X$  set to 25, 75, or 100 MeV. The background is described by a second-order Chebychev function for the  $RM_{\gamma D_s^+}$  and a flipped Argus function [53] for the  $RM_\gamma$ . The signal events in the  $KK\pi$  ( $N_{KK\pi}$ ) mode and in the  $K_S^0 K$  ( $N_{K_S^0 K}$ ) mode are correlated by

$$N_{K_S^0 K} = f_{sig} \cdot N_{KK\pi}, \quad (1)$$

$$f_{sig} = \frac{\epsilon_{K_S^0 K} \cdot \mathcal{B}(D_s^+ \rightarrow K_S^0 K^+) \cdot \mathcal{B}(K_S^0 \rightarrow \pi^+ \pi^-)}{\epsilon_{KK\pi} \cdot \mathcal{B}(D_s^+ \rightarrow K^+ K^- \pi^+)}, \quad (2)$$

where  $\epsilon_{K_S^0 K}$  and  $\epsilon_{KK\pi}$  are the efficiencies of event selection in the  $K_S^0 K$  and  $KK\pi$  modes, while  $\mathcal{B}(D_s^+ \rightarrow K_S^0 K^+) = (1.450 \pm 0.035)\%$  and  $\mathcal{B}(D_s^+ \rightarrow K^+ K^- \pi^+) = (5.37 \pm 0.10)\%$  are the branching fractions for  $D_s^+$  decaying to  $K_S^0 K^+$  and  $K^+ K^- \pi^+$ , respectively;  $\mathcal{B}(K_S^0 \rightarrow \pi^+ \pi^-) = (69.20 \pm 0.05)\%$  represents the branching fraction of  $K_S^0$  to  $\pi^+ \pi^-$  [43]. Figure 4 shows the fit results with  $\Gamma_X$  set to 50 MeV at  $\sqrt{s} = 4.682$  GeV. The obtained signal yields are listed in Table I for each data sample, along with the corresponding statistical significance determined by variations in likelihoods and degrees of freedom with and without the signal.

Since the largest significance of the signal among all c.m. energies is  $3.5\sigma$  at  $\sqrt{s} = 4.682$  GeV, we determine the upper limits of the number of signal events  $N_{KK\pi}^{UL}$  at each energy point. Utilizing the Bayesian method [54], the likelihood distribution  $L(x)$  is determined by repeating the fit changing the number of expected signal events. The upper limits at 90% confidence level (C.L.) are determined by the equation  $\int_0^{N_{KK\pi}^{UL}} L(x) dx / \int_0^\infty L(x) dx = 0.9$ . The upper limits of the Born cross section for  $e^+e^- \rightarrow \gamma X$  multiplied by the branching fraction of  $X \rightarrow D_s^+ D_{s1}^-(2536)$  is calculated by

$$\sigma^{UL} \cdot \mathcal{B} = \frac{N_{KK\pi}^{UL}}{\mathcal{L}_{int} \cdot (1 + \delta) \cdot \frac{1}{|1 - \Pi|^2} \cdot \epsilon_{KK\pi} \cdot \mathcal{B}_1 \cdot \mathcal{B}_2}, \quad (3)$$

where  $\mathcal{L}_{int}$  is the integrated luminosity at each energy point,  $1 + \delta$  is the ISR correction factor based on the QED calculation with 1% accuracy [55] and obtained from the KKMC generator,  $\frac{1}{|1 - \Pi|^2}$  is the vacuum polarization factor (VP) from Ref. [56],  $\mathcal{B}_1 = (5.37 \pm 0.10)\%$  [43] and  $\mathcal{B}_2 = (35.9 \pm 5.9)\%$  [52] are the branching fractions for the  $D_s^+ \rightarrow K^+ K^- \pi^+$  and  $D_{s1}^-(2536) \rightarrow \bar{D}^{*0} K^-$  decays.

The upper limits of the product of the cross section and branching fraction  $\sigma(e^+e^- \rightarrow \gamma X) \cdot \mathcal{B}(X \rightarrow D_s^+ D_{s1}^-(2536) + c.c.)$  determined at 90% C.L., as well as the other input values, are shown in Table I, where only the statistical uncertainty is considered.

## VI. SYSTEMATIC UNCERTAINTIES

The sources of systematic uncertainties in the determination of the upper limits of the Born cross-sections  $\sigma^{UL} \cdot \mathcal{B}$  are classified into two categories: the multiplicative terms and the additive terms.

### A. Multiplicative systematic uncertainties

The multiplicative uncertainties include tracking, PID,  $K_S^0$  reconstruction, photon reconstruction, range requirements for  $M_{K+\pi^-}$ ,  $M_{K+K^-}$ ,  $M_{\pi+\pi^-}$ ,  $M_{K+K^- \pi^+ / K_S^0 K^+}$  and  $RM_{\gamma D_s^+ K^-}$ , VP factor, luminosity, branching fractions of intermediate states, physical model, kinematic fit, and  $(1 + \delta) \cdot \epsilon_{KK\pi}$ .

The systematic uncertainty for tracking is assigned to be 1.0% for each  $\pi/K$  track [57], while the uncertainty for PID is assigned to be 1.0% [57].

We quote 2.0% as the systematic uncertainty caused by  $K_S^0$  reconstruction, based on Ref. [57], in which the same  $K_S^0$  reconstruction method is applied.

The uncertainty due to photon detection efficiency is determined to be 1.0% per photon [51], according to a study using as control sample  $J/\psi \rightarrow \rho\pi$  events.

The systematic uncertainties due to the range requirements on  $M_{K+\pi^-}$ ,  $M_{K+K^-}$ , and  $M_{K+K^- \pi^+}$  for the  $KK\pi$  mode, and on  $M_{\pi+\pi^-}$  and  $M_{K_S^0 K^+}$  for the  $K_S K$  mode, stem from the resolution difference between data and MC and are determined by comparing the signal shapes of data and MC; they are found to be 1.2%, < 0.1% (negligible), 0.2%, 0.3%, and 0.6%, respectively. Since a simultaneous fit is performed in this analysis, only the uncertainties associated with  $M_{K+\pi^-}$ ,  $M_{K+K^-}$ , and  $M_{K+K^- \pi^+}$  contribute to the global multiplicative uncertainty, even though all of them affect the correlation coefficient  $f_{sig}$ . Since no significant signal is observed in the recoil mass of  $\gamma D_s^+ K^-$  in data, a different method is employed to study the systematic uncertainty from the  $RM_{\gamma D_s^+ K^-}$  mass window requirement; we smear the  $\gamma$  energy distribution by a Gaussian with 1% uncertainty and reconstruct the smeared recoil mass  $RM_{\gamma D_s^+ K^-}^{smear}$ . The difference in efficiency by applying the same requirement in

TABLE I. The values used to determine  $\sigma(e^+e^- \rightarrow \gamma X) \cdot \mathcal{B}(X \rightarrow D_s^+ D_{s1}^- (2536))$ . Only the statistical uncertainty is presented, and the mass and width of the  $X$  candidate are set to be 4.503 GeV/ $c^2$  and 0.05 GeV, respectively.  $\mathcal{L}_{int}$  is the integral luminosity,  $(1 + \delta)$  is the radiative correction factor,  $\frac{1}{|1-\Pi|^2}$  is the VP factor,  $\epsilon_{KK\pi}$  ( $\epsilon_{K_S^0 K}$ ) is the selection efficiency of the  $KK\pi$  ( $K_S^0 K$ ) mode,  $N_{KK\pi}$  is the number of signal events for the  $KK\pi$  mode obtained by fitting,  $S$  is the statistical significance of the signal,  $N_{KK\pi}^{UL}$  is the upper limit of the number of signals at 90% C.L., and  $\sigma^{UL} \cdot \mathcal{B}$  is the upper limit of the product of the cross-section and the branching fraction at 90% C.L.

$\sqrt{s}$ (GeV)	$\mathcal{L}_{int}$ (pb $^{-1}$ )	$(1 + \delta)$	$\frac{1}{ 1-\Pi ^2}$	$\epsilon_{KK\pi}$ (%)	$\epsilon_{K_S^0 K}$ (%)	$N_{KK\pi}$	$S$	$N_{KK\pi}^{UL}$	$\sigma^{UL} \cdot \mathcal{B}$ (pb)
4.612	103.7	0.689	1.055	4.47	8.04	$0.0_{-0.0}^{+0.4}$	$0.1\sigma$	1.7	26.8
4.628	521.5	0.734	1.054	4.27	7.66	$0.6_{-0.7}^{+1.3}$	$0.1\sigma$	2.8	8.6
4.641	551.7	0.751	1.054	4.03	7.36	$1.4_{-1.0}^{+1.8}$	$1.8\sigma$	5.4	16.0
4.661	529.4	0.773	1.054	2.60	4.61	$0.0_{-0.0}^{+0.6}$	$0.3\sigma$	2.8	13.1
4.682	1667.4	0.785	1.054	3.58	6.12	$7.0_{-2.8}^{+3.5}$	$3.5\sigma$	12.5	13.1
4.699	535.5	0.793	1.054	4.34	7.83	$2.2_{-1.3}^{+1.6}$	$2.1\sigma$	5.6	15.0
4.740	163.9	0.808	1.055	4.82	8.63	$0.0_{-0.0}^{+0.4}$	$1.1\sigma$	1.9	15.0
4.750	366.6	0.811	1.055	4.75	8.86	$0.5_{-1.3}^{+2.2}$	$0.3\sigma$	4.3	15.1
4.781	511.5	0.821	1.055	4.92	9.15	$0.0_{-0.0}^{+0.5}$	$0.9\sigma$	2.0	4.9
4.843	525.2	0.835	1.056	4.51	8.64	$0.0_{-0.0}^{+0.4}$	$0.1\sigma$	1.8	4.6
4.918	207.8	0.845	1.056	4.79	8.95	$2.0_{-1.2}^{+1.8}$	$2.2\sigma$	5.1	30.0
4.951	159.3	0.851	1.056	4.68	8.71	$0.0_{-0.0}^{+0.4}$	$0.1\sigma$	1.7	13.5

TABLE II. The requirements on the modified recoiling mass  $RM'_{D^{*0}}$  and on the  $\chi^2$  of the 2C kinematic fit for each mode and energy set.

Variables/Sets	I	II	III
$RM'_{D^{*0}}$ for $KK\pi$ (MeV/ $c^2$ )	(1999.9, 2034.9)	(1999.9, 2029.9)	(1993.9, 2041.9)
$RM'_{D^{*0}}$ for $K_S^0 K$ (MeV/ $c^2$ )	(2001.9, 2021.9)	(1997.9, 2033.9)	(1994.9, 2041.9)
$\chi^2$ in $KK\pi$	< 12.4	< 16.4	< 8.4
$\chi^2$ in $K_S^0 K$	< 20.4	< 23.2	< 12.4

TABLE III. The multiplicative systematic uncertainties associated with  $KK\pi$  mode, expressed as percentages.

$\sqrt{s}$ (GeV)	4.612	4.628	4.641	4.661	4.682	4.699	4.74	4.75	4.781	4.843	4.918	4.951
Tracking	4.0	4.0	4.0	4.0	4.0	4.0	4.0	4.0	4.0	4.0	4.0	4.0
PID	4.0	4.0	4.0	4.0	4.0	4.0	4.0	4.0	4.0	4.0	4.0	4.0
$\gamma$ reconstruction	1.0	1.0	1.0	1.0	1.0	1.0	1.0	1.0	1.0	1.0	1.0	1.0
$M_{K^+\pi^-}$ range	1.2	1.2	1.2	1.2	1.2	1.2	1.2	1.2	1.2	1.2	1.2	1.2
$M_{K^+K^-\pi^+}$ range	0.2	0.2	0.2	0.2	0.2	0.2	0.2	0.2	0.2	0.2	0.2	0.2
$RM_{\gamma D_s^+ K^-}$ range	0.7	0.7	0.7	0.7	0.7	0.7	0.7	0.7	0.7	0.7	0.7	0.7
VP	0.1	0.1	0.1	0.1	0.1	0.1	0.1	0.1	0.1	0.1	0.1	0.1
Luminosity	1.0	1.0	1.0	1.0	1.0	1.0	1.0	1.0	1.0	1.0	1.0	1.0
$\mathcal{B}(D_s^+ \rightarrow K^+ K^- \pi^+)$	1.9	1.9	1.9	1.9	1.9	1.9	1.9	1.9	1.9	1.9	1.9	1.9
$\mathcal{B}(D_{s1}^- (2536) \rightarrow \bar{D}^{*0} K^-)$	16.4	16.4	16.4	16.4	16.4	16.4	16.4	16.4	16.4	16.4	16.4	16.4
Physical model	3.6	3.6	3.6	3.6	3.6	3.6	3.6	3.6	3.6	3.6	3.6	3.6
Kinematic fit	5.8	6.2	8.1	4.7	5.5	3.4	3.0	3.1	3.1	7.6	6.7	6.9
$(1 + \delta) \cdot \epsilon_{KK\pi}$	0.5	0.4	0.8	3.0	3.3	5.5	4.8	6.0	6.9	4.3	4.2	4.9
Total	18.8	19.0	19.7	18.8	19.0	19.1	18.8	19.2	19.5	19.9	19.6	19.8

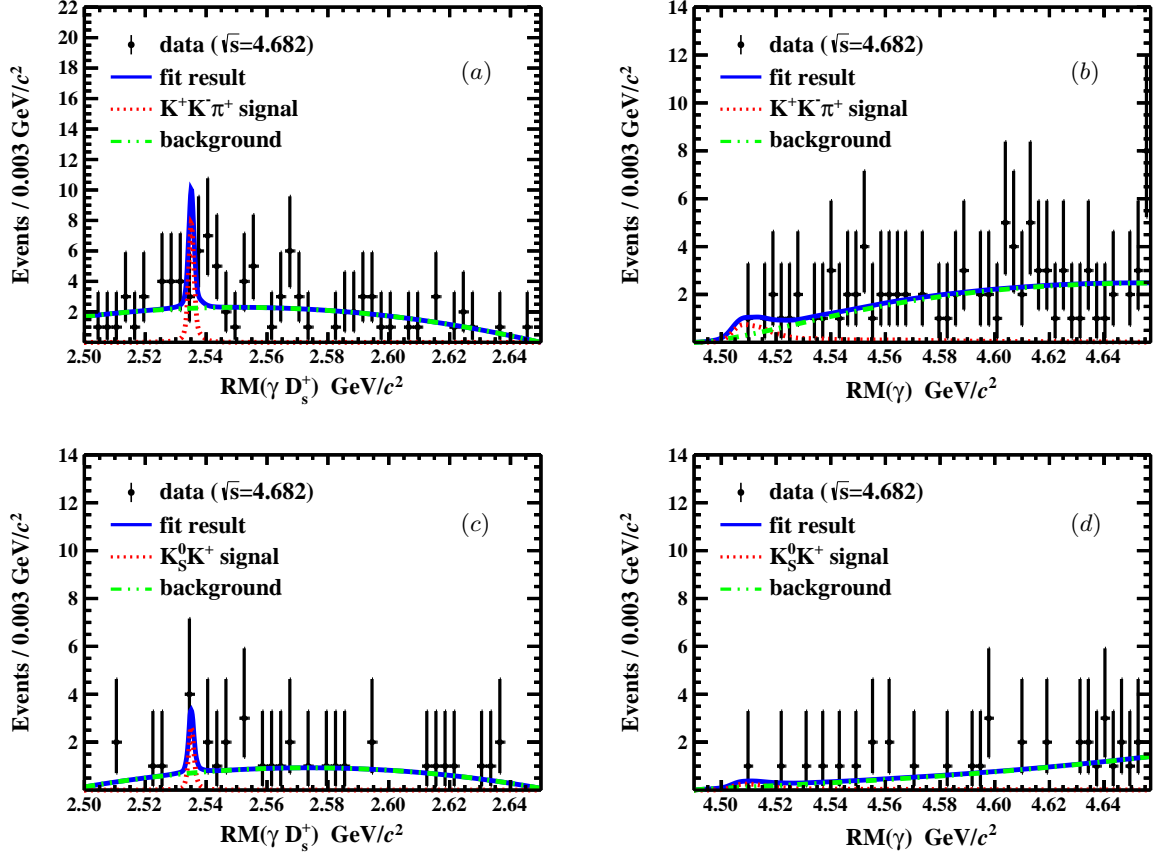


FIG. 4. The results of the two-dimensional simultaneous fit at  $\sqrt{s} = 4.682$  GeV, where (a) and (b) are the projected distributions of the  $\gamma D_s^+$  recoiling mass and of the  $\gamma$  recoiling mass for the  $KK\pi$  mode, while (c) and (d) are for the  $K_S^0 K$  mode. Dots with error bars indicate data, blue solid curves indicate the best fit results, red dashed lines indicate the  $D_{s1}^-$  (2536) and  $X$  signals, and the green dashed lines indicate the backgrounds.

TABLE IV. The uncertainties of the correlation coefficient  $\Delta(f_{sig})$  evaluated at each energy point, expressed as percentages.

$\sqrt{s}$ (GeV)	4.612	4.628	4.641	4.661	4.682	4.699	4.740	4.750	4.781	4.843	4.918	4.951
tracking	2.0	2.0	2.0	2.0	2.0	2.0	2.0	2.0	2.0	2.0	2.0	2.0
PID	2.0	2.0	2.0	2.0	2.0	2.0	2.0	2.0	2.0	2.0	2.0	2.0
$K_S^0$ reconstruction	2.0	2.0	2.0	2.0	2.0	2.0	2.0	2.0	2.0	2.0	2.0	2.0
Physical model	4.8	4.8	4.8	4.8	4.8	4.8	4.8	4.8	4.8	4.8	4.8	4.8
$M_{K+\pi^-}$ range	1.2	1.2	1.2	1.2	1.2	1.2	1.2	1.2	1.2	1.2	1.2	1.2
$M_{\pi^+\pi^-}$ range	0.3	0.3	0.3	0.3	0.3	0.3	0.3	0.3	0.3	0.3	0.3	0.3
$M_{K+K^-\pi^+}/K_S^0 K^+$ range	0.6	0.6	0.6	0.6	0.6	0.6	0.6	0.6	0.6	0.6	0.6	0.6
$RM_{\gamma D_s^+ K^-}$ range	0.7	0.7	0.7	0.7	0.7	0.7	0.7	0.7	0.7	0.7	0.7	0.7
Kinematic fit	5.5	5.8	7.6	4.7	5.2	3.3	2.9	3.1	3.0	8.4	8.2	6.5
$\mathcal{B}(D_s^+ \rightarrow K_S^0 K^+)$	2.4	2.4	2.4	2.4	2.4	2.4	2.4	2.4	2.4	2.4	2.4	2.4
$\mathcal{B}(K_S^0 \rightarrow \pi^+\pi^-)$	0.1	0.1	0.1	0.1	0.1	0.1	0.1	0.1	0.1	0.1	0.1	0.1
$\mathcal{B}(D_s^+ \rightarrow K^+ K^- \pi^+)$	1.9	1.9	1.9	1.9	1.9	1.9	1.9	1.9	1.9	1.9	1.9	1.9
Total	8.8	9.0	10.2	8.3	8.6	7.6	7.5	7.5	7.5	10.8	10.7	9.5

the  $RM_{\gamma D_s^+ K^-}$  and  $RM_{\gamma D_s^+ K^-}^{smear}$  distributions is taken as the related systematic uncertainty. We assign 0.7% and 0.2% for the range requirement of  $RM_{\gamma D_s^+ K^-}$  in  $KK\pi$  mode and  $K_S^0 K$  mode, respectively.

The uncertainty from the vacuum polarization factor is less than 0.1% [56].

The integrated luminosity is measured using Bhabha events, with an uncertainty of about 1.0% at each energy

point [35].

The systematic uncertainties associated with the branching fractions  $\mathcal{B}(D_s^+ \rightarrow K^+K^-\pi^+)$ ,  $\mathcal{B}(D_s^+ \rightarrow K_S^0K^+)$ ,  $\mathcal{B}(K_S^0 \rightarrow \pi^+\pi^-)$ , and  $\mathcal{B}(D_{s1}^-(2536) \rightarrow \bar{D}^{*0}K^-)$  are quoted as 1.9% [43], 2.4% [43], 0.1% [43], and 16.4% [52], respectively.

The uncertainty associated with the physical model of the  $e^+e^- \rightarrow \gamma X$  process is estimated by changing the PHSP to a helicity amplitude (HELAMP) model [42] when generating the signal MC sample. The differences in efficiency between the PHSP and the HELAMP model, 3.6% for the  $KK\pi$  mode and 3.1% for the  $K_S^0K$  mode, are considered as systematic uncertainties. The PHSP model, which results with a lower efficiency, is adopted as the nominal model for a conservative measurement.

To study the systematic uncertainty caused by the kinematic fit, we correct the helix parameters of charged tracks in the MC simulation [58]. The efficiency difference with and without the helix correction, as shown in Table III, is taken as the systematic uncertainty.

In the nominal results, the detection efficiencies and ISR corrections  $(1 + \delta) \cdot \epsilon_{KK\pi}$  are obtained from MC sample, with the cross-section line shape described by  $E_\gamma^3/s$ . The uncertainty from the input cross-section line shape is estimated by using the Breit-Wigner function of the  $Y(4660)$  state instead. The changes in the resultant Born cross-sections, shown in Table III, are taken as the systematic uncertainty from the  $(1 + \delta) \cdot \epsilon_{KK\pi}$  term.

Based on Eq. 3, all the multiplicative systematic uncertainties associated with the  $KK\pi$  mode for each energy point are listed in Table III, and the total systematic uncertainties are obtained by adding them in quadrature assuming no correlation among all the sources. To take into account the multiplicative systematic uncertainties in the upper limit calculation, the normalized likelihood distributions are smeared with a Gaussian function with a mean of  $\epsilon_{KK\pi}$  and a standard deviation of  $\delta_\epsilon^{abs} = \epsilon_{KK\pi} \cdot \delta_\epsilon^{rel}$ , where  $\delta_\epsilon^{abs}$  and  $\delta_\epsilon^{rel}$  are the absolute and relative multiplicative systematic uncertainties, respectively. The smeared likelihood is defined as

$$L(N_{KK\pi}) = \int_0^1 L' \left( \frac{\epsilon}{\epsilon_{KK\pi}} N_{KK\pi} \right) \frac{1}{\sqrt{2\pi}\delta_\epsilon^{abs}} e^{-\frac{(\epsilon - \epsilon_{KK\pi})^2}{2\delta_\epsilon^{abs}}} d\epsilon. \quad (4)$$

### B. Additive systematic uncertainties

The additive systematic uncertainties arise from the fit process and mainly include the uncertainties associated with the background shape and the correlation coefficient  $f_{sig}$ , which is related to the efficiency ratio  $\epsilon_{K_S^0K}/\epsilon_{KK\pi}$ , as well as the branching fractions  $\mathcal{B}(D_s^+ \rightarrow K_S^0K^+)$ ,  $\mathcal{B}(K_S^0 \rightarrow \pi^+\pi^-)$ , and  $\mathcal{B}(D_s^+ \rightarrow K^+K^-\pi^+)$ .

We estimate the systematic uncertainty from background shape by using a first-order Chebyshev function instead of the second-order Chebyshev function in the

$RM_{\gamma D_s^+}$  projection, and a second-order Chebyshev function instead of the anti-Argus function [53] in the  $RM_\gamma$  projection to describe the background shapes. The highest upper limit of the variations in the background shapes is assigned as the associated systematic uncertainty.

We account for the systematic uncertainty arising from the efficiency ratio  $\epsilon_{K_S^0K}/\epsilon_{KK\pi}$  and the branching fractions  $\mathcal{B}(D_s^+ \rightarrow K_S^0K^+)$ ,  $\mathcal{B}(K_S^0 \rightarrow \pi^+\pi^-)$ , and  $\mathcal{B}(D_s^+ \rightarrow K^+K^-\pi^+)$  in the simultaneous fit, employing the same method as the multiplicative systematic uncertainties in Section VI A. Note that the uncertainties associated with tracking and PID, which contribute to the efficiency ratio  $\epsilon_{K_S^0K}/\epsilon_{KK\pi}$ , are partially correlated; therefore, their effects are partially canceled. The uncertainties related to the  $\gamma$  reconstruction are fully canceled out. Other uncertainty sources of the efficiency ratio  $\epsilon_{K_S^0K}/\epsilon_{KK\pi}$  associated with the physical model, mass interval requirement, and kinematic fit are considered as independent in the two modes. All the uncertainties from different sources are treated as independent, and the total systematic uncertainty of  $f_{sig}$  is obtained by summing them in quadrature. The systematic uncertainties from  $f_{sig}$  at each energy point are presented in Table IV. We incorporate the  $f_{sig}$  and its related uncertainty at each energy point in the simultaneous fit, adopting the highest upper limit as the value considering the associated systematic uncertainty.

After considering the systematic uncertainties, Table V and Fig. 5 represent the upper limits of the product of the cross-section and the branching fraction  $\sigma(e^+e^- \rightarrow \gamma X) \cdot \mathcal{B}(X \rightarrow D_s^+ D_{s1}^-(2536) + c.c.)$ , assuming  $\Gamma_X$  is 25 MeV, 50 MeV, 75 MeV, or 100 MeV.

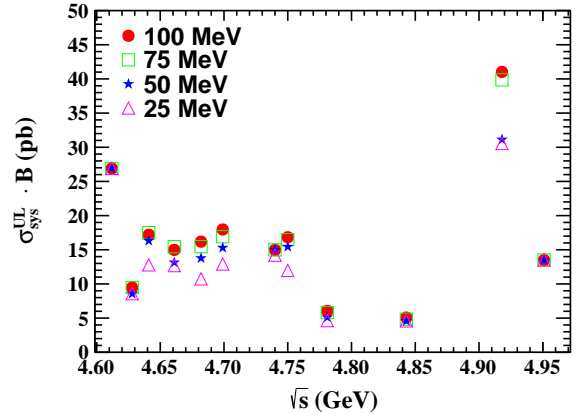


FIG. 5. The upper limits of the product of the cross section and branching fraction  $\sigma(e^+e^- \rightarrow \gamma X) \cdot \mathcal{B}(X \rightarrow D_s^+ D_{s1}^-(2536) + c.c.)$  at each energy points assuming the width  $\Gamma_X = 25, 50, 75, \text{ or } 100$  MeV at 90% C.L..

TABLE V. The results of  $\sigma(e^+e^- \rightarrow \gamma X) \cdot \mathcal{B}(X \rightarrow D_s^+ D_{s1}^-(2536) + c.c.)$  under different assumptions of  $X$ 's width ( $\Gamma_X = 25, 50, 75, 100$  MeV) including the systematic uncertainties. The  $N_{KK\pi}^{UL'}$  and  $\sigma_{sys}^{UL} \cdot \mathcal{B}$  values represent the upper limits of the number of signal events and of the product of the cross-section and branching fraction at 90% C.L.

$\Gamma_X$	25 MeV		50 MeV		75 MeV		100 MeV	
$\sqrt{s}$ (GeV)	$N_{KK\pi}^{UL'}$	$\sigma_{sys}^{UL} \cdot \mathcal{B}$ (pb)						
4.612	1.7	26.9	1.7	26.9	1.7	26.9	1.7	26.9
4.628	2.8	8.6	2.8	8.6	3.1	9.5	3.1	9.5
4.641	4.3	12.8	5.5	16.3	5.9	17.5	5.8	17.2
4.661	2.7	12.7	2.8	13.1	3.3	15.4	3.2	15.0
4.682	10.2	10.7	13.1	13.8	14.7	15.5	15.4	16.2
4.699	4.8	12.9	5.7	15.3	6.3	16.9	6.7	18.0
4.740	1.8	14.2	1.9	15.0	1.9	15.0	1.9	15.0
4.750	3.4	12.0	4.4	15.4	4.7	16.5	4.8	16.8
4.781	1.9	4.6	2.1	5.1	2.4	5.8	2.5	6.1
4.843	1.8	4.6	1.8	4.6	1.9	4.8	2.0	5.1
4.918	5.2	30.6	5.3	31.1	6.8	39.9	7.0	41.0
4.951	1.7	13.5	1.7	13.5	1.7	13.5	1.7	13.5

## VII. SUMMARY

Based on  $e^+e^-$  collision data at c.m. energies from 4.612 to 4.951 GeV collected by the BESIII spectrometer, corresponding to an integrated luminosity of  $5.8 \text{ fb}^{-1}$ , the exotic molecular state  $X$  ( $J^{PC} = 1^{-+}$ ) is searched for the first time via the process  $e^+e^- \rightarrow \gamma X, X \rightarrow D_s^+ D_{s1}^-(2536)$ . No significant signal is observed and the upper limits of  $\sigma(e^+e^- \rightarrow \gamma X) \cdot \mathcal{B}(X \rightarrow D_s^+ D_{s1}^-(2536))$  are determined at 90% C.L., assuming  $M_X = 4.503 \text{ GeV}/c^2$  and  $\Gamma_X = 25, 50, 75, \text{ or } 100 \text{ MeV}$ . The obtained upper limits are shown in Table V and Fig. 5. These upper limits range from 5 pb to 45 pb, while typically 15 pb around 4.68 GeV. Assuming the total cross section of  $e^+e^- \rightarrow Y(4660)$  is about 300 pb [43] and the branching fraction of  $Y(4660) \rightarrow \gamma X$  being 0.1% (same to  $\mathcal{B}(Y(4260) \rightarrow \gamma X')$  estimated in Ref. [34], where  $X'$  decays into non-strange D meson pairs), the product of the cross-section and the branching fraction is 0.3 pb, which is 50 times lower than the upper limit determined in this analysis. At  $\sqrt{s} = 4.682 \text{ GeV}$ , there is evidence of a signal with  $3.5\sigma$  significance when  $\Gamma_X = 50 \text{ MeV}$ . However, this evidence may only be a local and statistical fluctuation. Therefore, more experimental data are needed to confirm or exclude it by considering the global significance and the systematic uncertainties.

## ACKNOWLEDGMENTS

The BESIII Collaboration thanks the staff of BEPCII and the IHEP computing center for their strong support. This work is supported in part by National

Key R&D Program of China under Contracts Nos. 2020YFA0406300, 2020YFA0406400, 2023YFA1606000; National Natural Science Foundation of China (NSFC) under Contracts Nos. 12275058, 11635010, 11735014, 11935015, 11935016, 11935018, 12025502, 12035009, 12035013, 12061131003, 12192260, 12192261, 12192262, 12192263, 12192264, 12192265, 12221005, 12225509, 12235017, 12361141819; the Chinese Academy of Sciences (CAS) Large-Scale Scientific Facility Program; the CAS Center for Excellence in Particle Physics (CCEPP); Joint Large-Scale Scientific Facility Funds of the NSFC and CAS under Contract No. U1832207; 100 Talents Program of CAS; The Institute of Nuclear and Particle Physics (INPAC) and Shanghai Key Laboratory for Particle Physics and Cosmology; German Research Foundation DFG under Contracts Nos. FOR5327, GRK 2149; Istituto Nazionale di Fisica Nucleare, Italy; Knut and Alice Wallenberg Foundation under Contracts Nos. 2021.0174, 2021.0299; Ministry of Development of Turkey under Contract No. DPT2006K-120470; National Research Foundation of Korea under Contract No. NRF-2022R1A2C1092335; National Science and Technology fund of Mongolia; National Science Research and Innovation Fund (NSRF) via the Program Management Unit for Human Resources & Institutional Development, Research and Innovation of Thailand under Contracts Nos. B16F640076, B50G670107; Polish National Science Centre under Contract No. 2019/35/O/ST2/02907; Swedish Research Council under Contract No. 2019.04595; The Swedish Foundation for International Cooperation in Research and Higher Education under Contract No. CH2018-7756; U. S. Department of Energy under Contract No. DE-FG02-05ER41374

- 
- [1] For recent reviews, see N. Brambilla, S. Eidelman, C. Hanhart, A. Nefediev, C. P. Shen, C. E. Thomas, A. Vairo and C. Z. Yuan, *Phys. Rept.* **873**, 1 (2020); F. K. Guo, C. Hanhart, U. G. Meißner, Q. Wang, Q. Zhao and B. S. Zou, *Rev. Mod. Phys.* **90**, 015004 (2018); H. X. Chen, W. Chen, X. Liu and S. L. Zhu, *Phys. Rept.* **639**, 1 (2016); N. Brambilla *et al.*, *Eur. Phys. J. C* **71**, 1534 (2011).
- [2] S. K. Choi *et al.* [Belle Collaboration], *Phys. Rev. Lett.* **91**, 262001 (2003).
- [3] D. Acosta *et al.* [CDF Collaboration], *Phys. Rev. Lett.* **93**, 072001 (2004).
- [4] V. M. Abazov *et al.* [D0 Collaboration], *Phys. Rev. Lett.* **93**, 162002 (2004).
- [5] B. Aubert *et al.* [BaBar Collaboration], *Phys. Rev. D* **71**, 071103 (2005).
- [6] E. S. Swanson, *Phys. Lett. B* **588**, 189 (2004).
- [7] L. Zhao, L. Ma, and S. L. Zhu, *Phys. Rev. D* **89**, 094026 (2014).
- [8] L. Maiani, F. Piccinini, A. D. Polosa, and V. Riquer, *Phys. Rev. D* **71**, 014028 (2005).
- [9] N. N. Achasov and E. V. Rogozina, *Mod. Phys. Lett. A* **30**, 1550181 (2015).
- [10] M. Suzuki, *Phys. Rev. D* **72**, 114013 (2005).
- [11] Y. S. Kalashnikova, *Phys. Rev. D* **72**, 034010 (2005).
- [12] M. Takizawa and S. Takeuchi, *Prog. Theor. Exp. Phys.* **2013**, 093D01 (2013).
- [13] B. Aubert *et al.* [BaBar Collaboration], *Phys. Rev. Lett.* **95**, 142001 (2005).
- [14] T. E. Coan *et al.* [CLEO Collaboration], *Phys. Rev. Lett.* **96**, 162003 (2006).
- [15] C. Z. Yuan *et al.* [Belle Collaboration], *Phys. Rev. Lett.* **99**, 182004 (2007).
- [16] S. R. Xue, H. J. Jing, F. K. Guo, and Q. Zhao, *Phys. Lett. B* **779**, 402 (2018).
- [17] W. Qin, S. R. Xue, and Q. Zhao, *Phys. Rev. D* **94**, 054035 (2016).
- [18] G. J. Ding, *Phys. Rev. D* **79**, 014001 (2009).
- [19] E. Kou and O. Pene, *Phys. Lett. B* **631**, 164-169 (2005).
- [20] S. L. Zhu, *Phys. Lett. B* **625**, 212 (2005).
- [21] J. Z. Wang, D. Y. Chen, X. Liu and T. Matsuki, *Phys. Rev. D* **99**, 114003 (2019).
- [22] D. Y. Chen, X. Liu and T. Matsuki, *Eur. Phys. J. C* **78**, 136 (2018).
- [23] B. Q. Li and K. T. Chao, *Phys. Rev. D* **79**, 094004 (2009).
- [24] F. J. Llanes-Estrada, *Phys. Rev. D* **72**, 031503 (2005).
- [25] M. Ablikim *et al.* [BESIII], *Phys. Rev. Lett.* **110**, 252001 (2013).
- [26] D. R. Thompson *et al.* [E852 Collaboration], *Phys. Lett. B* **205**, 397 (1988).
- [27] S. U. Chung *et al.* [E852 Collaboration], *Phys. Rev. D* **60**, 092001 (1999).
- [28] G. S. Adams *et al.* [E852 Collaboration], *Phys. Lett. B* **657**, 27 (2007).
- [29] A. Abele *et al.* [Crystal Barrel Collaboration], *Phys. Lett. B* **423**, 175 (1998).
- [30] A. Abele *et al.* [Crystal Barrel Collaboration], *Phys. Lett. B* **446**, 349 (1999).
- [31] E. I. Ivanov *et al.* [E852 Collaboration], *Phys. Rev. Lett.* **86**, 3977 (2001).
- [32] Yu. A. Khokhlov *et al.* [VES Collaboration], *Nucl. Phys. A* **663**, 596c (2000).
- [33] M. Ablikim *et al.* [BESIII Collaboration], *Phys. Rev. Lett.* **129**, 192002 (2022).
- [34] Q. Wang, *Phys. Rev. D* **89**, 114013(2014).
- [35] M. Ablikim *et al.* [BESIII Collaboration], *Chin. Phys. C* **11**, 113003 (2022).
- [36] M. Ablikim *et al.* [BESIII Collaboration], *Nucl. Instrum. Methods A* **614**, 345 (2010).
- [37] M. Ablikim *et al.* [BESIII Collaboration], *Chin. Phys. C* **44**, 040001 (2020).
- [38] X. Li *et al.*, *Radiat. Detect. Technol. Methods* **1**, 13 (2017); Y. X. Guo *et al.*, *Radiat. Detect. Technol. Methods* **1**, 15 (2017); P. Cao *et al.*, *Nucl. Instrum. Methods A* **953**, 163053 (2020).
- [39] S. Agostinelli *et al.* [GEANT4 Collaboration], *Nucl. Instrum. Methods A* **506**, 250 (2003).
- [40] K. X. Huang, *et al.*, *Nucl. Sci. Tech.* **33**, 142 (2022).
- [41] S. Jadach, B. F. L. Ward and Z. Was, *Phys. Rev. D* **63**, 113009 (2001); *Chin. Phys. C* **130**, 260 (2000).
- [42] D. J. Lange, *Nucl. Instrum. Methods A* **462**, 152 (2001); R. G. Ping, *Chin. Phys. C* **32**, 599 (2008).
- [43] S. Navas *et al.* [Particle Data Group], to be published in *Phys. Rev. D* **110**, 030001 (2024).
- [44] J. C. Chen, G. S. Huang, X. R. Qi, D. H. Zhang and Y. S. Zhu, *Phys. Rev. D* **62**, 034003 (2000); R. L. Yang, R. G. Ping and H. Chen, *Chin. Phys. Lett.* **31**, 061301 (2014).
- [45] E. R. Was, *Phys. Lett. B* **303**, 163 (1993).
- [46] R. E. Mitchell *et al.* [CLEO Collaboration], *Phys. Rev. D* **79**, 072008 (2009).
- [47] M. Ablikim *et al.* [BESIII Collaboration], *Phys. Rev. D* **104**, 012016 (2021).
- [48] P. del A. Sanchez *et al.* [BaBar Collaboration], *Phys. Rev. D* **83**, 052001 (2011).
- [49] M. Ablikim *et al.* [BESIII Collaboration], *Phys. Rev. D* **110**, 032017 (2024).
- [50] G. Punzi, arXiv:2011.11770.
- [51] M. Ablikim *et al.* [BESIII Collaboration], *Phys. Rev. D* **104**, 032012 (2021).
- [52] M. Ablikim *et al.* [BESIII Collaboration], arXiv:2407.07651
- [53] H. Albrecht *et al.* [ARGUS Collaboration], *Phys. Lett. B* **241**, 278 (1990).
- [54] J. Conrad *et al.*, *Phys. Rev. D* **67**, 012002 (2003).
- [55] E. A. Kuraev and V. S. Fadin, *Yad. Fiz.* **41**, 733 (1985).
- [56] F. Jegerlehner, *Nuovo Cim. C* **034S1**, 31-40 (2011).
- [57] M. Ablikim *et al.* [BESIII Collaboration], *Phys. Rev. Lett.* **126**, 102001 (2021).
- [58] M. Ablikim *et al.* [BESIII Collaboration], *Phys. Rev. D* **87**, 012002 (2013).